The Suitability of the Three-way Catalyst for Hydrogen Fuelled Engines

Yavuz, Mustafa; Brinklow, George; Cova Bonillo, Alexis; Herreros, Martin; Wu, Dawei; Doustdar, Omid; Zeraati Rezaei, Soheil; Tsolakis, Athanasios; Millington, Paul; Alcove Clave, Silvia

DOI:
10.1595/205651324X17054113843942

Document Version
Peer reviewed version

Citation for published version (Harvard):
Yavuz, M, Brinklow, G, Cova Bonillo, A, Herreros, M, Wu, D, Doustdar, O, Zeraati Rezaei, S, Tsolakis, A, Millington, P & Alcove Clave, S 2024, 'The Suitability of the Three-way Catalyst for Hydrogen Fuelled Engines', *Johnson Matthey Technology Review*, vol. 68, no. 3. https://doi.org/10.1595/205651324X17054113843942

JOHNSON MATTHEY
TECHNOLOGY REVIEW

technology.matthey.com

Johnson Matthey's international journal of research exploring science and technology in industrial applications

**********Accepted Manuscript**********

This article is an accepted manuscript

It has been peer reviewed and accepted for publication but has not yet been copyedited, house styled, proofread or typeset. The final published version may contain differences as a result of the above procedures

It will be published in the **July 2024** issue of the *Johnson Matthey Technology Review*

Please visit the website https://technology.matthey.com/ for Open Access to the article and the full issue once published

Johnson Matthey Technology Review
Johnson Matthey Plc
Orchard Road
Royston
SG8 5HE
UK
Tel +44 (0)1763 253 000
Email tech.review@matthey.com

<Doi: 10.1595/205651324X17054113843942>

<First page: TBC>

The Suitability of the Three-way Catalyst for Hydrogen Fuelled Engines

A study in carbon emissions reduction and NO_x management

M. Yavuz, G. Brinklow, A. Cova Bonillo, J.M. Herreros, D. Wu, O. Doustdar, S. Zeraati-Rezaei, A. Tsolakis*

Department of Mechanical Engineering, University of Birmingham, Edgbaston, B15 2TT, UK

P. Millington, S. Alcove Clave

Johnson Matthey, Blount's Court, Sonning Common, Reading, RG4 9NH, UK

Email: * a.tsolakis@bham.ac.uk

<Article history>

Received 5th October 2023; Revised 9th January 2024; Accepted 15th January 2024; Online 16th January 2024

<End of article history>

Abstract

This experimental study investigates the palladium/rhodium based three-way catalytic converter (TWC) in a H_2 - gasoline dual-fuel spark ignition (SI) engine under stoichiometric and lean conditions. The work focused on lean-burn engine operating conditions with the aim of reducing NO_X emissions during the combustion process, where the TWC is not effective, while improving the thermal efficiency of the engine. Under these lean-burn engine conditions, the combustion promoting properties of H_2 allowed for maintained engine combustion stability as determined by the COV_{imep} values even up to ultra lean conditions (λ=2.0). It was found that by reducing the combustion temperature through the application of lean conditions, engine out NO_X emissions could be reduced or even eliminated, while under these conditions the TWC was effective in reducing engine-out carbon-based gaseous emissions.

Keywords: H_2, Lean Burn, Aftertreatment, Dual-fuel, SI Engine

1. Introduction

Decarbonisation of the transportation sector is imperative if global CO_2 targets are going to be achieved. Even with optimistic projections, the global market share of electric vehicles (EVs) will still be less than 50 % by the year 2035 suggesting that alternative low- or zero-carbon fuels will be required to meet these targets [1].

Hydrogen (H_2) as a fuel is often portrayed as the panacea for the transportation sector due to there being no carbon-based emissions [2]. However, there are several drawbacks to the use of pure H_2 combustion within an internal combustion engine (ICE). These include production (at present most of the world's H_2 is produced through the reformation of fossil fuels [3]), storage both on and offboard a vehicle, concerns of knocking, increased NO_X emissions, and a lack of public acceptance [4][5][6]. One option to assist in the decarbonisation of the transportation sector in the medium term is the adoption of gasoline and H_2 dual-fuel spark ignition (SI) ICEs [2].

Previous studies have already investigated the performance of dual-fuelled gasoline and H_2 engines, focusing on engine efficiency and pre-aftertreatment emissions. Pan et al. investigated a gasoline/H_2 dual-fuel SI engine with a hydrogen energy share (HES) of 20 % and reported emissions and cylinder pressures. It was found that the addition of H_2 reduced combustion duration and increased NO_X emissions twofold, whilst CO and hydrocarbon (HC) emissions were reduced by approximately 50 % and 80 % respectively [7]. This increase in NO_X with a reduction in CO and HCs for gasoline/H_2 engines is well reported and found to increase as the HES increases with several papers concluding the same [2][8]. Wang et al. reported the same trend as the HES increased during engine start events [9]. Since the majority of NO_X emissions produced from H_2 combustion are formed through the thermal NO_X pathway several studies have reported that leaner combustion, thus reducing the flame temperature can manage NO_X emissions. Du et al. reported that engine out NO_X emissions from gasoline/H_2 combustion with

Doi: 10.1595/205651324X17054113843942

20 % HES could be reduced from over 5,000 ppm to 1,000 ppm by operating at a lambda of 1.5 [10]. Du et al. also found that both CO and HC emissions reduced at a lambda of 1.5. Results from Wang et al. at a lambda of 1.4 were in agreement with Du et al. other than a reported increase in HC emissions [11]. Suresh and Porpatham found that by operating at a lambda of 2.0 with a HES of 10 % the NO_X emissions could be reduced by approximately 95 % [12].

Further to the effect on pre-aftertreatment emissions, the addition of H_2 to gasoline combustion has been reported to act as a combustion promoter due to its increased laminar flame velocity and wider flammability limits when compared to gasoline [13]. Elsemary et al. reported an increase in brake thermal efficiency (BTE) as the HES was increased from 0 % to 30 % with a reduction in BTE as the HES was increased beyond 30 % [14]. Other studies also found there to be an optimal H_2 ratio for BTE of between 20 % - 30 % [8]. Yet, Niu et al. reported a contrasting monotonic increase in BTE as the H_2 ratio was increased to 50 % [15]. This was due to the H_2 being directly injected, whereas studies that injected H_2 through port fuel injection (PFI) suffered a volumetric efficiency reduction at HES values greater than 30 % resulting in the drop in BTE. Further to the effect on pre-aftertreatment emissions, the addition of H_2 to gasoline combustion has been reported to act as a combustion promoter due to its increased laminar flame velocity and wider flammability limits when compared to gasoline [13]. Under some ICE lean-burn operating conditions, BTE can be increased thus reducing CO_2 emissions [16]. Also, H_2's wider flammability limit can allow a H_2-gasoline dual-fuelled SI engine to run at leaner conditions than those possible with only gasoline combustion.

The current state-of-the-art aftertreatment device for gasoline ICEs is the three-way catalyst (TWC), so called because of its ability to simultaneously convert CO, NO_X and HC whilst above the catalyst light-off temperature, with combustion taking place at or around stoichiometry. As new combustion systems are developed, new aftertreatment systems will need to be developed to meet emission regulations. Whilst pre-aftertreatment emissions have been widely reported, a gap has been identified in the literature for the application of catalytic aftertreatment systems to gasoline/H_2 dual-fuel ICEs. Therefore, this work investigates a modern TWC under dual-fuelled gasoline-H_2 ICE operating under stoichiometric and lean engine conditions to understand the applicability of the TWC to this future combustion system. The novelty of this work is provided by the focus on combining a lean-burning gasoline-H_2 engine with a modern catalytic aftertreatment system.

Doi: 10.1595/205651324X17054113843942

2. Methodology

2.1. Experimental setup

For this experimental study, work was conducted using a modern gasoline direct injection (GDI) SI engine (details in Table 1). The engine was modified to feature injection of H_2 (industrial purity) into the intake manifold. The injection strategy of the dual fuel engine set up required using the engine's direct injectors to inject gasoline with the injection timing set to -267 CAD aTDC whilst the flow rate of H_2 was controlled with a calibrated H_2 volumetric flow meter. The TWC provided by Johnson Matthey PLC was located in a close coupled catalyst (CCC) location in keeping with modern trends. The TWC featured a cordierite monolith with 600 cpsi and a total platinum group metal (PGM) loading of 30 g/ft^3 with a ratio of palladium to rhodium of 23:7. Before testing, the TWC was de-greened in a furnace at a temperature of 600 °C.

Table 1. Test engine specification.

Parameter	Specification
Number of Cylinders	3
Compression Ratio	11:1
Swept Volume	1.5 L
Bore	84 mm
Stroke	90 mm
Rated Power	134 kW @ 6000 rpm
Rated Torque	240 Nm @ 1600-4500 rpm

Emissions measurement before and after the TWC for NO_X, CO, HCs, CO_2, H_2O, N_2O and NH_3 were taken using an MKS 2030 Fourier transform infrared (FTIR) spectrometer. For H_2 emissions, a V&F HSense electron impact ionisation mass spectrometer (EIMS) was used. The TWC was also instrumented with k-type thermocouples to measure inlet and outlet gas temperatures and the monolith temperatures on the inlet and outlet face. Engine control and data were logged using ATI Vision software whilst combustion was analysed using an in-cylinder pressure transducer and crank angle encoder. The schematic for the test set up is shown in Figure 1.

Doi: 10.1595/205651324X17054113843942

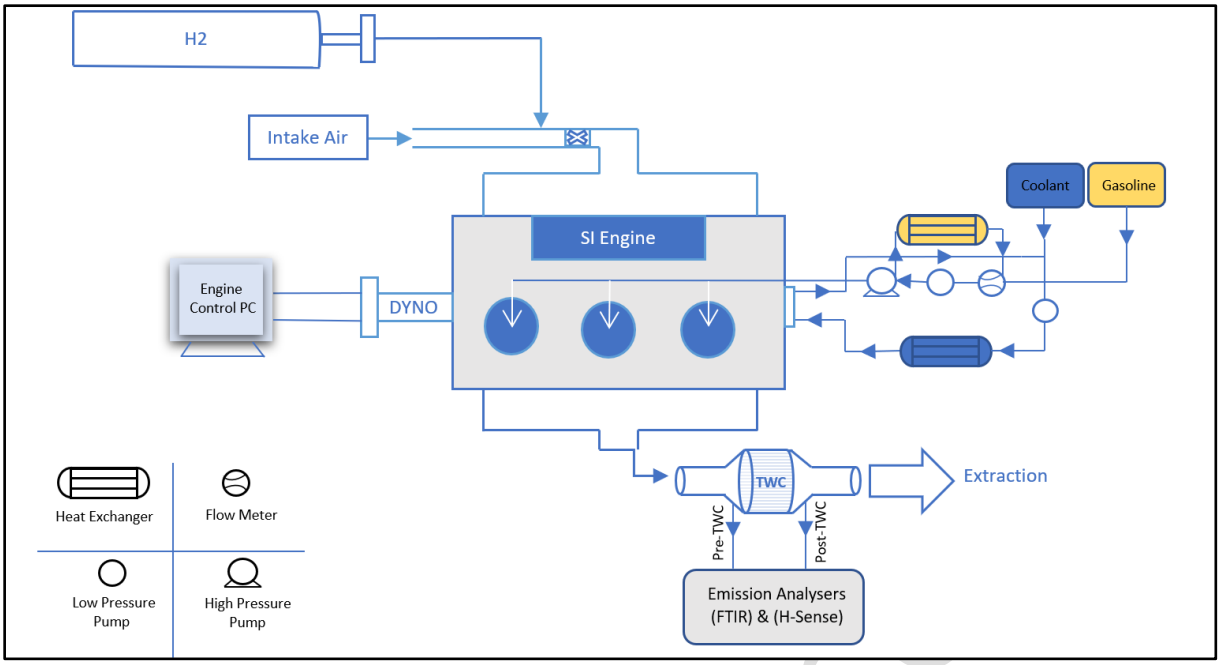

Figure 1. Engine test schematic set up.

2.2. Testing methodology

All tests were conducted at steady-state (speed/load) engine conditions as shown in Table 2. The engine torque was kept at 40 Nm and the engine speed at 2000 rpm while the lambda was varied between 1.0 and 1.2 for the baseline gasoline 0% HES and between 1.0 and 2.0 for the 12% HES dual-fuel combustion. This was decided based upon the combustion stability which was monitored using the cycle-to-cycle variation (COV_{imep}). This was maintained at less than 5% as variation in engine operation greater than this will negatively impact engine life and may cause fluctuations in combustion/performance that will inhibit the focused study of TWC performance. The engine lambda was adjusted automatically by the ECU through adjustment of the injection duration and throttle angle in order to increase air flow and maintain engine brake torque.

Table 2. Engine testing conditions.

Engine Speed / rpm	Engine Load / Nm	H_2 Energy Ratio / %	Lambda / [-]
2000	40	0	1.0 – 1.2
2000	40	12	1.0 – 2.0

The experiments started by using only gasoline and then dual-fuelled H_2-gasoline operation was adopted to study the effect of H_2 on emissions and engine performance. The properties of the fuels used in this study are reported in Table 3.

Doi: 10.1595/205651324X17054113843942

Table 3. H_2 and gasoline fuel properties [2] [17][18].

Properties	Hydrogen	Gasoline	Unit
Chemical Formula	H_2	C_7H_{17}	-
Molecular Weight	2	100-114	g/mol
Density	0.08	737	kg/m^3
Auto-ignition Temperature	585	371	°C
Minimum Ignition Energy	0.02	0.25	mJ
Lower Heating Value	120	43.44	MJ/kg
Stoichiometric Air-Fuel Ratio	34.2	14.7	kg air/ kg fuel
Quenching Gap @ NTP	0.64	~2	mm
Flammability Limits	4-75 (lean to rich)	1.4-7.6 (lean to rich)	% vol.

During this study, the HES was maintained at 12%. After H_2 injection, the lambda could be extended to 2.0 due to the wider flammability limits of H_2. The 12% HES combustion did not require any major hardware adjustments to the engine meaning that these results are applicable to commercial engines currently on the market. Lean combustion was studied due to the reduced fuel consumption at these conditions providing real world CO_2 savings. In order to make a comparison between the two combustion set ups and lambdas the MFB50 was maintained at between 3 and 4 CAD aTDC. This was achieved by adjusting the spark timing.

2.3. Calculation of COV_{imep}

In order to maintain engine durability, the combustion stability was monitored through the COV_{imep}. This was calculated over 200 cycles. The COV_{imep} was calculated as per Equation 1. The threshold value for an acceptable COV_{imep} was selected as 5%. This was because this value is the threshold for which it would become noticeable for the driver. It will also prevent damage to the engine due to the unstable operation at COV_{imep} values higher than this.

$$\mathrm{COV_{imep}} = \frac{\mathrm{stdev_{imep}}}{\mathrm{imep}} \text{ x } 100$$

Equation 1. Coefficient of variance for IMEP.

Doi: 10.1595/205651324X17054113843942

2.4. Calculation of TWC conversion efficiency

TWC performance was quantified by calculating the conversion efficiency. This was done using the gas concentrations measured at the inlet and outlet of the TWC. These were then used in Equation 2 for each emissions species to obtain the percentage of conversion achieved.

$$\eta_{\text{conversion}} = \frac{\text{Conc.}_{\text{inlet}} - \text{Conc.}_{\text{outlet}}}{\text{Conc.}_{\text{inlet}}} \text{ x } 100$$

Equation 2. Catalyst conversion efficiency.

2.5. Calculation of heat release rate

Heat release rate (HRR) was calculated based on the in-cylinder pressure measurement with respect to the crank angle degree. This was sampled using an in-cylinder pressure transducer and crank angle encoder. These were then converted to HRR with respect to crank angle degree using Equation 3 [19].

$$\frac{dQ}{d\theta} = \frac{\gamma}{\gamma - 1} P \frac{dV}{d\theta} + \frac{1}{\gamma - 1} V \frac{dP}{d\theta}$$

Equation 3. Calculation of heat release rate ($\frac{dQ}{d\theta}$) from in-cylinder pressure (P) and in-cylinder volume (V).

2.6. Calculation of brake thermal efficiency and brake specific fuel consumption

The BTE and brake specific fuel consumption (BSFC) were calculated using the brake power of the engine and the energy input to the engine from both the gasoline and the H_2. These are both shown in Equation 4 and Equation 5 respectively. In this case, ṁ is the mass flow rate (g/h), LHV is the lower heating value (kJ/g) and Ẇ is the engine brake power (kW).

$$\eta_{\text{BTE}} = \frac{\dot{W}_{\text{brake}}}{\left(\dot{m}_{\text{gasoline}} \text{ LHV}_{\text{gasoline}}\right) + \left(\dot{m}_{\text{hydrogen}} \text{ LHV}_{\text{hydrogen}}\right)}$$

Equation 4. Calculation of engine brake thermal efficiency for dual-fuel operation. In the case of pure gasoline operation, the mass flow rate of hydrogen was zero.

$$\text{BSFC} = \frac{\dot{m}_{\text{gasoline}} + \dot{m}_{\text{hydrogen}}}{\dot{W}_{\text{brake}}}$$

Equation 5. Calculation of brake specific fuel consumption for dual-fuel operation. In the case of pure gasoline operation, the mass flow rate of hydrogen was zero.

Doi: 10.1595/205651324X17054113843942

3. Results and Discussion

3.1. Combustion analysis

Figure 2 shows a comparison between 0% HES (dashed lines) and 12% HES (solid lines) for in-cylinder pressure (a) and HRR (b). For each lambda, the substitution of gasoline for H_2 caused an increase in peak cylinder pressure when compared to 0% HES. These increases in maximum pressure were 1.1, 1.8, and 2.0 bar, corresponding to a 3.6, 6.0, and 6.6 % increase in peak firing pressure at lambda 1.0, 1.1, and 1.2, respectively. This trend of increased peak cylinder pressure was amplified as lambda increased for the same HES. This was an effect of the increased intake manifold pressure resulting from the increased throttle angle the engine operated at to achieve the leaner combustion. This was evident for both 0 % HES and 12 % HES. The combustion process of the 12 % HES was advanced when compared to that of the 0 % HES at all lambda values. This was due to the combustion properties of H_2, specifically its lower minimum ignition energy and higher flame speed [20]. The addition of H_2 accelerated combustion, allowing more fuel to be burned in a shorter period, thereby releasing more energy in the same period.

The HRR (Figure 2b) shows that as lambda increased from 1.0 to 1.2 for the baseline 0 % HES case, the HRR and maximum heat release point (HRR_{max}) increased due to the combustion advance. This corresponds to the increase in the peak in-cylinder pressure. The HRR also showed a different trend for the 0 % HES and the 12 % HES. During the initial stages of combustion (-10 to -5 CAD aTDC) as shown in the zoomed section of Figure 2b, the 12 % HES HRR increased at a quicker rate than when compared to the 0 % HES. Then, after this initial increase in HRR for the 12 % HES it reduced, and the 0 % HES HRR caught up. This is most likely due to the available H_2 burning during the initial stage from -5 CAD aTDC to -10 CAD aTDC.

Doi: 10.1595/205651324X17054113843942

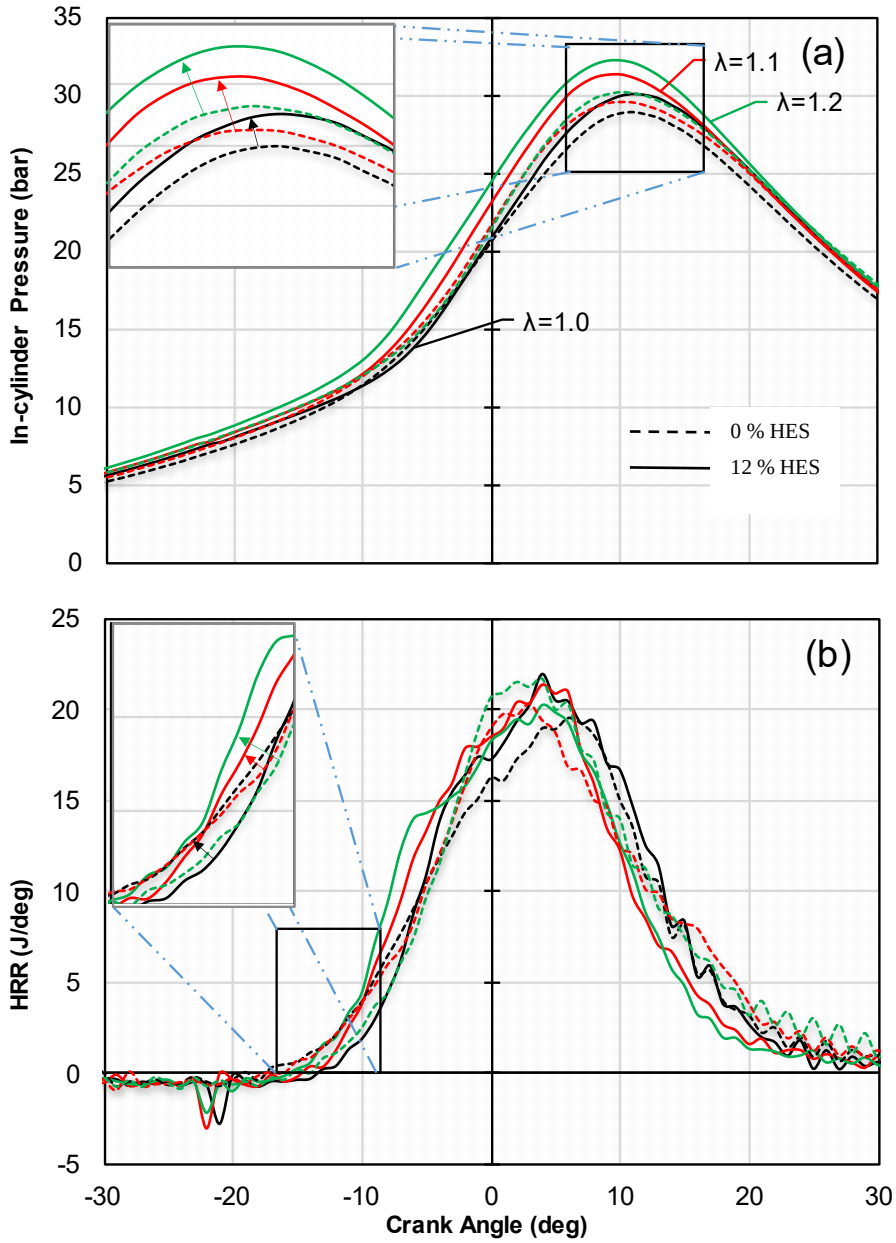

Figure 2. In-cylinder pressure (a) and heat release rate (b) with respect to the crank angle for 0% and 12% HES, for each lambda tested from 1.0 to 1.2. Please note that the negative HRR seen close to -20 CAD aTDC was related to noise from the spark signal.

Early heat release dominates for temperature rise effects. Therefore, it can be expected that the in-cylinder temperature was higher for the 12 % HES combustion. In addition to the earlier increase in HRR for the 12 % HES there was a reduction in combustion duration. This is evident in Figure 2b where the HRR curves reduce sooner compared to the 0% HES combustion. This was since H_2 burns faster and earlier due to the relatively quicker flame speed and higher diffusivity of H_2 respectively. Knocking was avoided by maintaining the angle of MFB50 constant through adjustment to the spark timing.

Doi: 10.1595/205651324X17054113843942

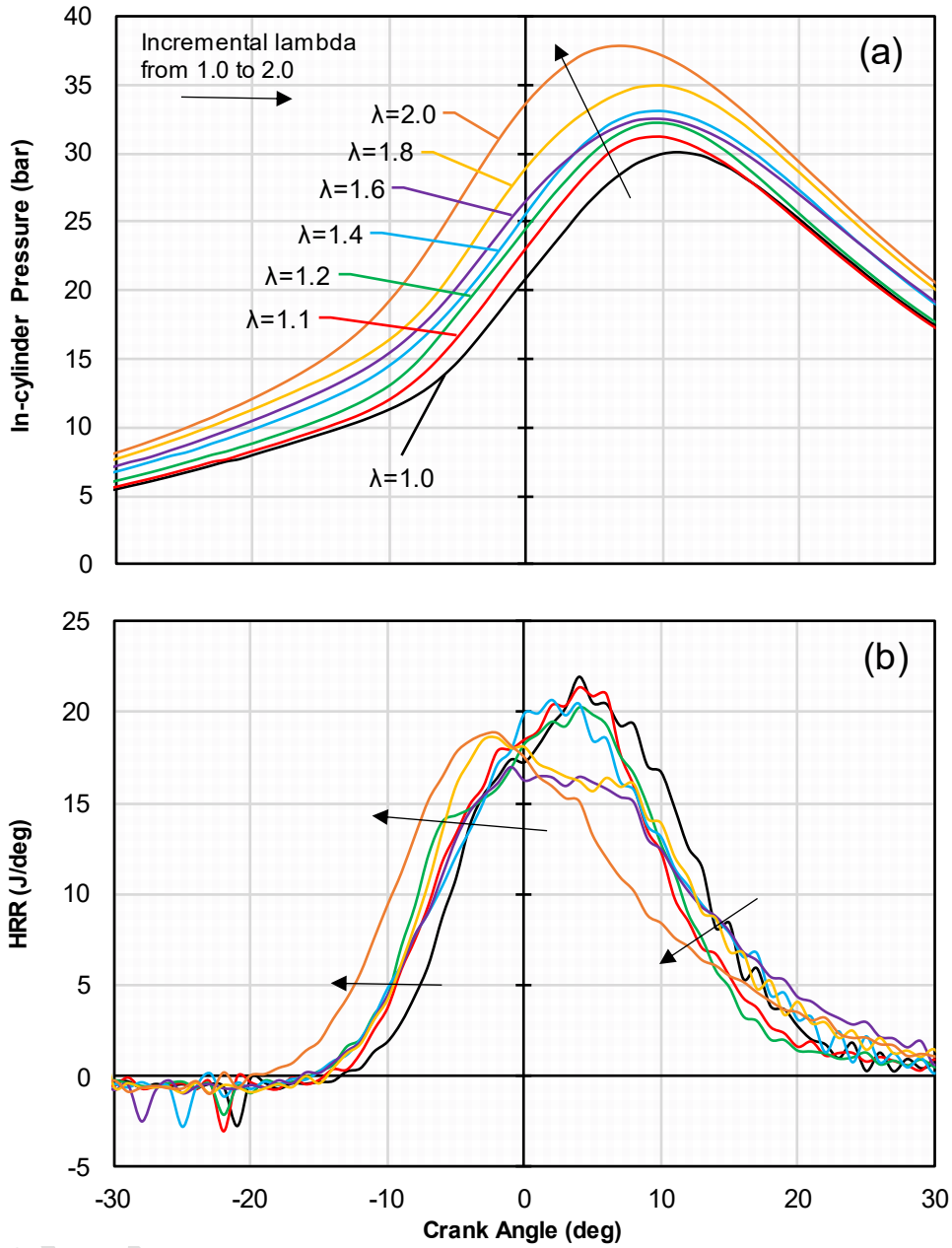

Figure 3. In-cylinder pressures (a) and net heat release rate (b) with respect to the crank angle for 12% HES at lambda values between 1.0 to 2.0. Please note that the negative HRR seen between -20 and -30 CAD aTDC was related to noise from the spark signal.

For reasons of engine stability, it was not possible to extend the operation of the engine using gasoline alone to conditions beyond lambda 1.2. In order to overcome this, the ability of H_2 to extend the flammability of these mixtures allowed for lean combustion beyond a lambda value of 1.2. Figure 3 shows in-cylinder pressure and HRR for lambda values 1.0 to 2.0 for 12 % HES. This allows for understanding of the effect of excess O_2 on the combustion of the mixture. As the mixture became leaner, the maximum in-cylinder pressure increased from 30 bar under stoichiometric conditions up to almost 38 bar at a lambda of 2.0. This was most likely a

Doi: 10.1595/205651324X17054113843942

combination of the advanced combustion enforced through the advancing of the spark timing to maintain MFB50 for each lambda, and the increase in intake manifold pressure at higher lambdas as discussed previously. It can be observed in Figure 3b that for lambda values of 1.8 and greater that the HRR occurred very early (before TDC) due to the advancement in spark timing to maintain the same MFB50. This is also reflected by the earlier in-cylinder pressure rise in Figure 3a. As a result, the subsequent expansion from the combustion process was inhibited leading to a reduction in combustion efficiency.

Figure 4 shows the COV_{imep}. Generally, a maximum COV of 5 % is accepted as an indication of stable combustion [21], [22]. The COV_{imep} for the 0 % HES tests were higher than the 12 % HES tests under all lambda values tested, even with the same combustion phasing. This was due to the combustion enhancing properties of H_2 which reduced the cycle-to-cycle variation [20]. Even at a lambda value of 1.0 the combustion enhancing properties of H_2 could be observed by the reduction in COV_{imep}. For the 0 % HES experimental condition, the COV_{imep} reached 8 % for a lambda value of 1.2. As a result, the engine was not operated any leaner than this. Comparing the 12% HES combustion to the pure gasoline there was a clear improvement in combustion stability. This was due to the combustion enhancing properties of H_2 such as its high flame speed and wide flammability range which is reported elsewhere [23]. This also allowed combustion to continue to a lambda value of 2.0 whilst still maintaining a COV_{imep} of 2 %.

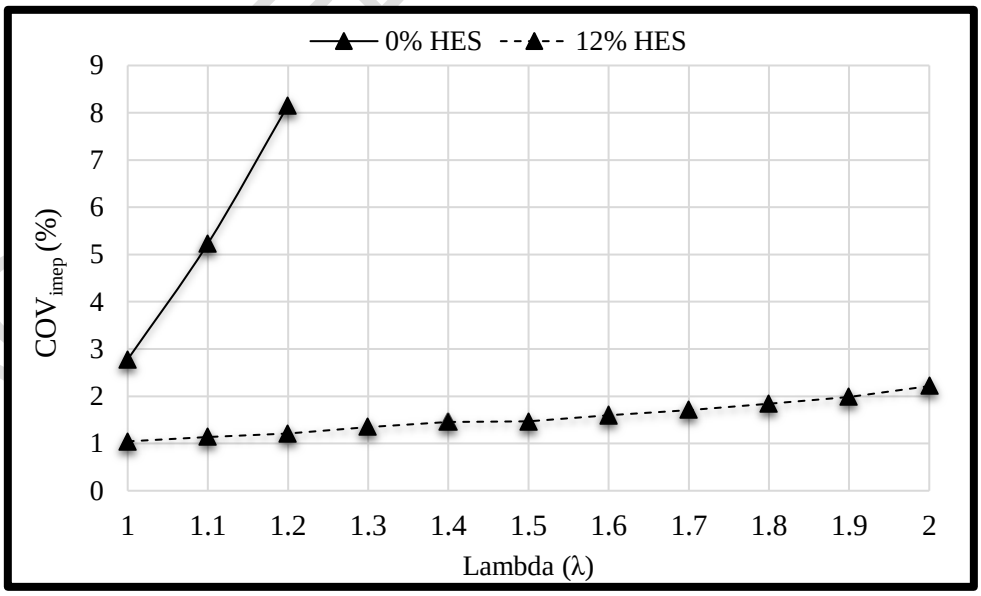

Figure 4. COV_{imep} from a lambda value of 1.0 to 2.0.

Doi: 10.1595/205651324X17054113843942

3.2. Performance Analysis

Lean operating conditions have been reported to improve BTE [24]. Figure 5a plots BTE with respect to lambda for both 0 % and 12 % HES. There was an increase in BTE of approximately 2 percentage points as lambda increased from 1.0 to 1.2 for the 0 % HES condition. This improvement in efficiency as lambda increases is well defined and linked to the reduction in combustion temperature reported with leaner flames limiting the temperature gradient between the combustion mixture and the cylinder walls [24]. This will result in a reduction of heat losses that allows for the extraction of more useable work from the fuel. Furthermore, as lambda was increased by opening the throttle to a larger angle there was a reduction in the pumping losses and an increase in volumetric efficiency. However, increasing lambda for the 12 % HES only resulted in a limited increase in efficiency of 0.1 percentage points as lambda increased from 1.0 to 1.2. This smaller increase was linked to the difference between port and direct injection. As the H_2 was port injected, the increase in efficiency afforded by the increased throttle opening was somewhat offset by the fact that the H_2 present in the intake manifold displaced some of the air. Yet, in the case of the directly injected gasoline, the increase in throttle angle related to a pure increase in volumetric efficiency. This was also reported by Gultekin et al. where negative effects on the volumetric efficiency for port injected H_2 ICEs were reported for HES ratios of 14 % or higher [25].

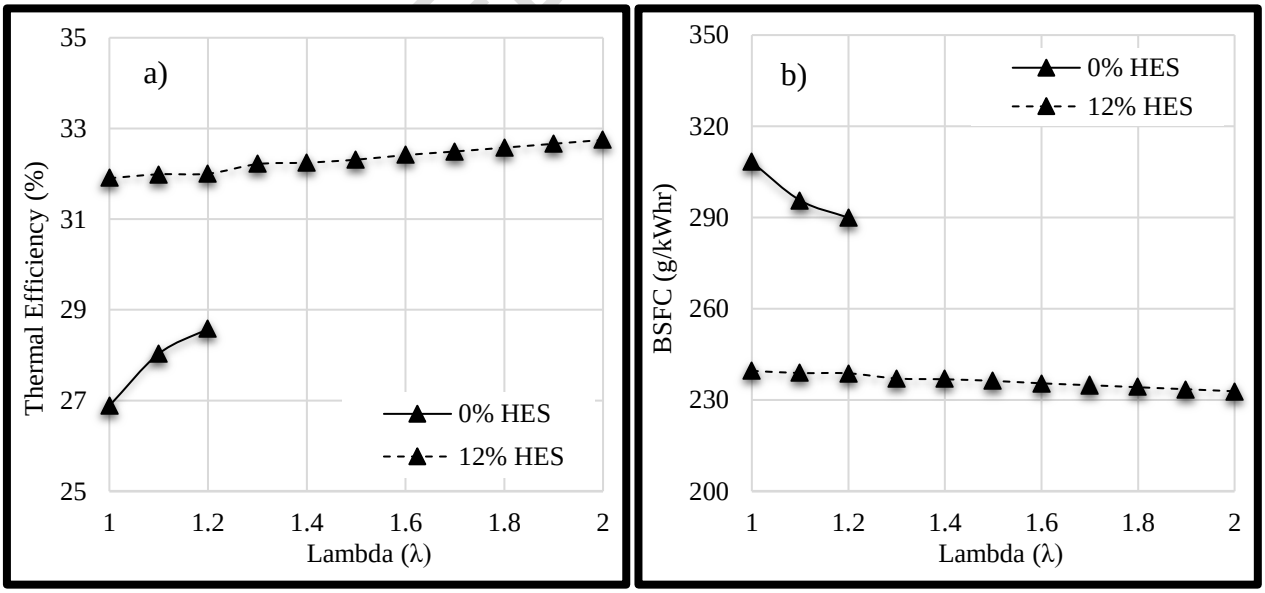

Figure 5. Brake thermal efficiency (a) and BSFC (b) values with respect to the lambda for the 0% and 12% HES test conditions.

When comparing the BTEs of 0 % and 12 % HES operation there was an increase of approximately 5 percentage points. This increase was a result of the improved combustion

Doi: 10.1595/205651324X17054113843942

properties of H_2 as discussed above leading to a reduced combustion duration/faster heat addition and therefore acting closer to the ideal thermodynamic cycle. It was also clear that the addition of H_2 improved BSFC. This was the effect of the increased BTE and higher energy density of H_2 per unit of mass meaning that less H_2 was required for the same fuel energy input to the system. This will lead to a reduction in mass based BSFC [26].

3.3. Emission Analysis

3.3.1. Engine-out Emissions

The use of H_2 to extend the lean combustion limit of the engine is of interest as it will also assist in the decarbonisation of the transport sector. By operating the engine at leaner conditions, it was possible to reduce the engine out CO_2 flow rate. Furthermore, the engine out emissions will vary based on the combustion in the cylinder which is greatly affected by the lambda value. These are shown in Figure 6 for a comparison between the 0 % and 12 % HES.

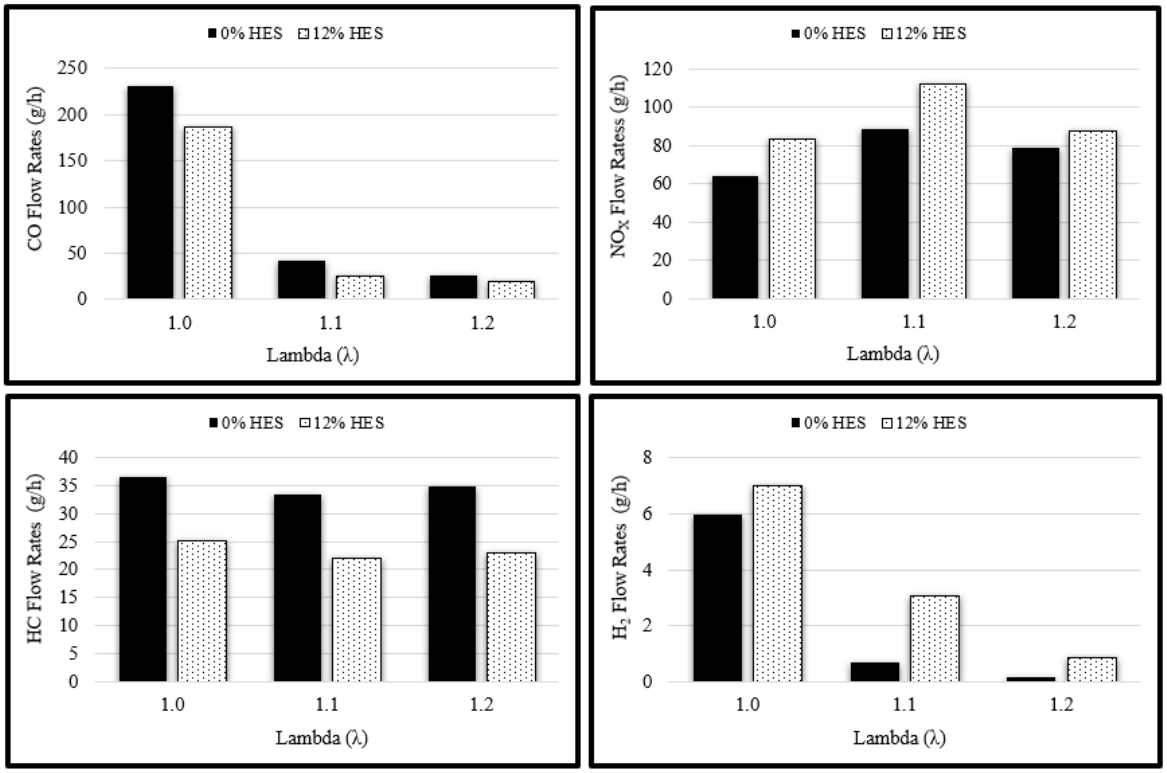

Figure 6. Engine out emissions concentrations for CO, NO_X, HC and H_2.

There was an observed reduction in CO and HC flow rates for the 12% HES case. This was a result of the reduced carbon content of the fuel. This reduction in CO and HC emissions was greater than the percentage reduction in fuel carbon content. This was a result of the combustion promoting properties of H_2 which increased the combustion efficiency therefore reducing CO

Doi: 10.1595/205651324X17054113843942

and HC further than just from the carbon replacement. As lambda increased there was a reduction in both CO and HCs for 0 % and 12 % HES. The effect on CO was greater than the effect on HCs. The reduction in CO and HCs as lambda increased was a result of the increased O_2 availability assisting in the complete oxidation of the fuel.

The addition of H_2 has both physical and chemical effects. The physical effect is due to the properties of H_2. The higher adiabatic flame temperature of H_2 increases the combustion chamber temperature, thereby increasing combustion efficiency and reducing unburned fuel. In addition, the amount of unburned gasoline on the inner wall surfaces of the cylinder will be reduced by the presence of H_2 due to the smaller flame quenching distance. The consumption of fuel begins with the H_2 abstraction reaction. This is shown in Eq. 6 where RH represents a generic gasoline molecule, M represents an abstracting element from the pool of radicals e.g. OH and R· represents an alkyl radical.

$$RH + M \rightarrow R\cdot + M + H\cdot \qquad \text{Eq. 6}$$

It can be noted that an alkyl radical is formed from Eq.6**Error! Reference source not found.**. This then enables the sequence of reactions that trigger the combustion process at low temperature (primary O_2 addition, isomerization, secondary O_2 addition, etc.) [27]. The increase in temperature, together with the supply of H_2, promotes the appearance of OH radicals as was shown by Fu et.al [28]. These are shown in Eq. 7 to Eq. 10:

$$H_2 + M \rightarrow 2H\cdot + M \qquad \text{Eq. 7}$$

It is possible that any H_2 present in the combustion chamber could be dissociated and turned into two H• radicals through impact with a third body (represented by M) as per Eq. 6. This H• radical can then lead to the formation of a hydroperoxyl radical (HO_2•) as per Eq. 8.

$$H\cdot + O_2 + M \rightarrow HO_2\cdot + M \qquad \text{Eq. 8}$$

The hydroperoxyl radical can then partake in the formation of hydroxyl radicals (OH•) which are the main radicals that will abstract H from the HC as shown in Eq. 6. This is done through Eq. 7. Furthermore, hydroxyl radical formation can also take place through the reaction of the H• radical with any H_2O present (Eq. 8). The increase in H_2 concentration for 12 % HES will assist this process further and reduce the HC emissions and improve combustion efficiency.

$$HO_2\cdot + CH_3\cdot \rightarrow OH\cdot + CH_3O \qquad \text{Eq. 7}$$

$$H\cdot + H_2O \rightarrow OH\cdot + H_2 \qquad \text{Eq. 8}$$

Doi: 10.1595/205651324X17054113843942

There was an increase in H_2 emissions from the engine for the 12 % HES case. This was expected due to the increased concentration of H_2 into the combustion chamber. Large concentrations of engine out H_2 is an indication of poor combustion efficiency. For future development of H_2 ICEs reduction of unburnt H_2 should be targeted. However, the presence of H_2 within the exhaust gas has been reported to have a positive effect on catalytic aftertreatment devices [29]. As lambda increased, there was a reduction in the engine out H_2 concentration. This was for the same reason as the reduction in engine out CO and HC emissions. This could be a potential control measure to manage the concentration of H_2 provided to any catalytic aftertreatment systems.

The major concern regarding H_2 ICE emissions is the formation of NO_X. This work shows that for stoichiometric combustion there was an increase in engine out NO_X concentration for the 12 % HES case. However, this was relatively small due to the low engine load tested. According to the literature, NO_x formation in H_2-assisted combustion occurs via the thermal pathway, i.e., through the Zeldovich mechanism [30], [31]. N_2 and O_2 react to form nitric oxide (NO) and atomic oxygen (O). The rate of NO and O production is faster due to the higher temperatures generated by the presence of H_2. The NO_X formation is a function of temperature and O_2 availability. As a result, the NO_X emissions increased when lambda was increased from 1.0 to 1.1 due to the increased availability of O_2. The engine out emissions for the 12 % HES combustion case from a lambda value of 1.0 to 2.0 are shown in Figure 7.

Doi: 10.1595/205651324X17054113843942

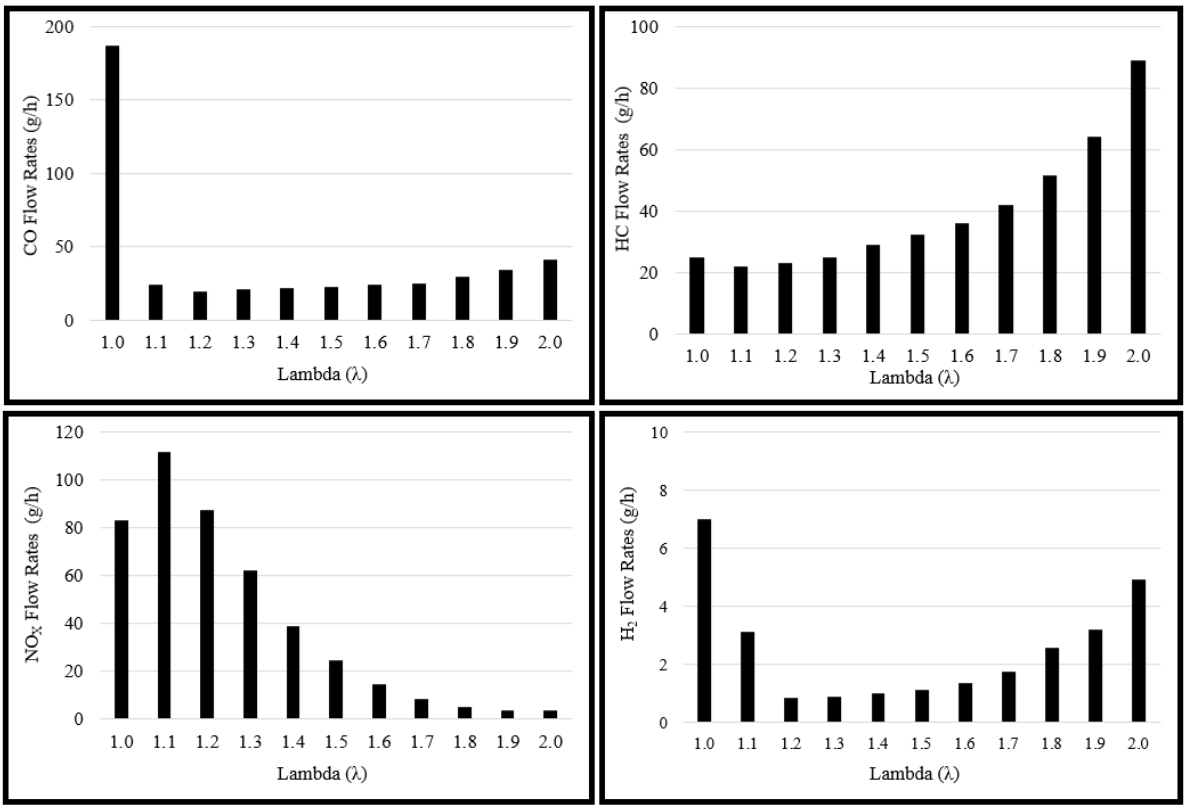

Figure 7. Engine out emissions for 12% HES including CO, NO_X, HC and H_2.

Engine out CO reduced substantially as lambda increased from 1.0 to 1.1. This is well understood as the increased availability of O_2 limits the amount of carbon that is only partly oxidised to CO rather than fully oxidised to CO_2. As lambda was increased beyond 1.1, there was limited change in engine out CO emissions. This suggests that after this lambda, any further increase in the O_2 concentration present for combustion had little to no effect in oxidising all carbon to CO_2. After an initial reduction in engine out HCs from a lambda value 1.0 to 1.2 there was a monotonic increase from 1.3 onwards. This resulted from the HC species present in the combustion. Whilst H_2 enhances combustion, there were still local areas within the combustion chamber beyond the lean combustion limit for gasoline where it will not combust and instead pass through to the exhaust gases [32]. As lambda was increased towards 1.4, the HC emissions increased beyond that of stoichiometric. This could be a potential challenge for the ultra-lean operation of gasoline-H_2 dual-fuel engines. It is expected that as the HES increases the challenge of HC emissions will be less critical.

The engine out NO_X emissions can be adjusted through changing lambda. The initial increase in engine out NO_X as lambda increased from 1.0 to 1.1 and 1.2 was a result of the increased O_2 availability. As lambda was increased further, there was a reduction in NO_X emissions due to the reduction in combustion temperature at leaner conditions. The reduction in NO_X reached a

Doi: 10.1595/205651324X17054113843942

point after a lambda value of 1.8 where NO_X emissions became negligible. Operating at a lambda of 1.8 or higher would limit the formation of NO_X such that it might be possible that an aftertreatment catalyst for the reduction of NO_X may not be necessary. What the tuning of lambda for gasoline-H_2 dual-fuel combustion engines could allow for would be the optimisation of exhaust gas concentrations in order to assist catalytic aftertreatment devices in emissions abatement.

3.3.2. Three-way catalyst performance

The regulated emissions performance of the TWC is analysed below for each of the different lambda values tested. The effect of H_2 addition on the TWC performance is shown in Figure 8 for both the 0 % HES and 12 % HES cases between lambda values of 1.0 to 1.2.

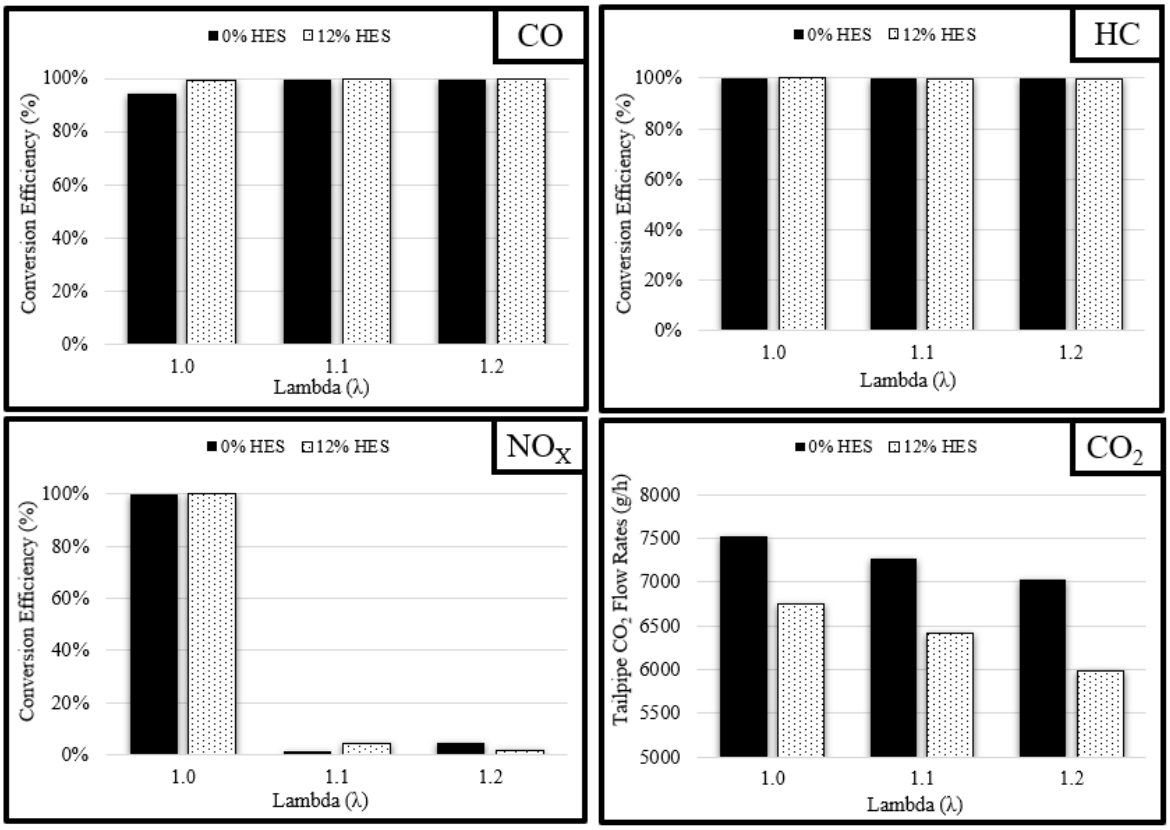

Figure 8. Comparison of TWC conversion for CO, NO_X and HCs including tailpipe mass flow rate of CO_2 for 0 % and 12 % HES

TWC performance was maintained for all conditions when comparing the performance of both 0 % and 12 % HES. As can be seen in Figure 8, CO and HC conversion was improved for lambda values from 1.0 to 1.2 under 0% HES and 12% HES operation. However, whilst the TWC converted approximately 100 % of the NO_x emissions under stoichiometric conditions, the performance under lean-burn operating conditions was poor with approximately 8 %

Doi: 10.1595/205651324X17054113843942

conversion under 12 % HES combustion. There was improved conversion over the TWC for operation under 12 % HES due to the increased H_2 availability which contributed to the reduction of NO_X [33]. The improvement in CO and HC emissions could be a result of increased H_2 before the TWC. It has been reported that H_2 availability before the TWC can aid the conversion of CO and HC [29].

The reduction in tailpipe CO_2 for the gasoline-H_2 combustion was expected due to the reduction in overall carbon content of the fuel. The combustion of the gasoline-H_2 mixture provided not only improved TWC CO conversion but also reduced total CO_2 emissions from the engine. The reduction in CO_2 emissions as lambda increased is well understood and documented but these results provide evidence that further CO_2 reduction is possible through the combustion of leaner gasoline-H_2 mixtures as the CO_2 concentration reduced as the lambda value was increased. However, at leaner conditions the TWC performance was inhibited as it was not able to reduce NO_X in the highly oxidative environment presented to the TWC. As lean combustion has been proposed as a solution towards limiting the NO_X emissions from an engine fuelled or co-fuelled with H_2 the performance of the TWC was tested under these conditions. The conversion performance for the 12 % HES experimental condition is shown in Figure 9 for lambda values from 1.0 to 2.0.

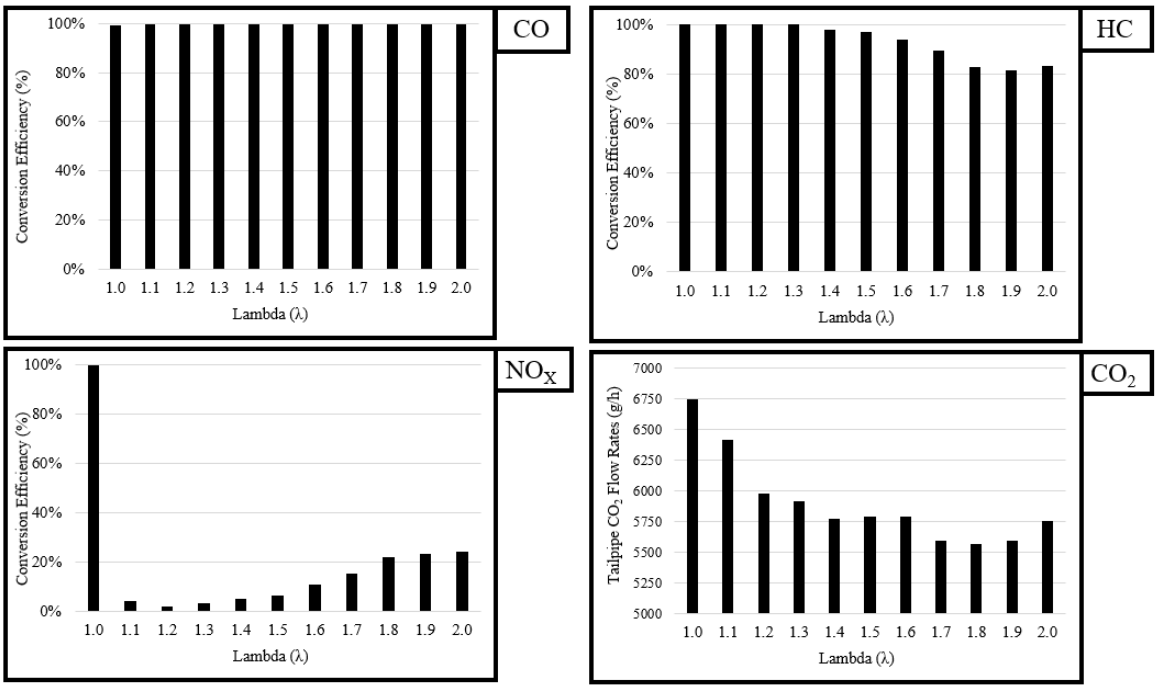

Figure 9. TWC conversion efficiency for CO, NO_X and HCs and tailpipe CO_2 concentration depending on the lambda values from 1.0 to 2.0 for 12% HES test condition.

Doi: 10.1595/205651324X17054113843942

The use of lean combustion for gasoline-H_2 dual-fuelled combustion presents a challenge for the conversion of NO_X and HCs over a TWC. NO_X conversion efficiency reduced at lambda values of 1.1 and higher as expected. This was due to the excess O_2 available before the TWC which oxidised the CO, H_2 and HC species that are used for the reduction of NO_X [34]. HC conversion efficiency was maintained as lambda increased from 1.0 to 1.6. However, beyond this there was a further reduction in HC conversion efficiency as the O_2 concentration increased at lambda values of 1.7 or greater. This has been reported to occur in rhodium catalysts due to the competition of O_2 and HCs for active sites on the rhodium [35]. The conversion of CO was maintained across the entire lambda range with the only change being the increase in conversion efficiency when lambda was increased from 1.0 to 1.1 as the excess O_2 provided an oxidising environment for the CO.

There was a constant drop in tailpipe CO_2 concentration as lambda was increased. This demonstrates there is sufficient scope for the use of dual-fuelled gasoline-H_2 engines as a means to decarbonise the transport sector in the medium term. The current TWC aftertreatment system was sufficient for the conversion of CO. However, ultra-lean conditions require additional measures to address NO_X and HC conversion. It is a possibility that by increasing the HES that emissions of HCs from the engine would be reduced. This will limit the demand placed on the TWC for HC oxidation. Furthermore, at ultra-lean conditions the NO_X emissions from the ICE were very low with only 43 ppm of NO_X at a lambda of 2.0.

The application of a TWC to a gasoline-H_2 dual-fuelled ICE shows promising results for the emissions control of THCs and CO, at both stoichiometric and lean conditions. However, the challenge with the application of a TWC at ultra-lean conditions is the slip of HCs. By operating the engine at a lambda of 1.8 there is a trade-off in NO_X and HC post-TWC concentrations. This condition could be promising when considering the use of a TWC for future gasoline-H_2 fuelled engines. In applications where there is increased availability for onboard H_2 storage the H_2 energy replacement ratio could be increased further. This would also reduce the HC emissions.

4. Conclusions

In this experimental study, a three-cylinder direct injection gasoline SI engine was operated at various lambdas whilst studying a blend of gasoline-H_2 with a 12 % HES. This work aimed to assess the applicability of current state of the art TWC aftertreatment to a gasoline-H_2 dual-fuel

Doi: 10.1595/205651324X17054113843942

engine at a range of different lambda conditions. Emissions of CO, NO_X and HCs were all reported whilst CO_2 reductions were also discussed.

The key findings have shown that the TWC is applicable for gasoline-H_2 dual-fuel combustion at stoichiometric conditions and that CO conversion can be improved at a lambda of 1.0. However, as the combustion shifted towards the lean regime there was a reduction in NO_X conversion over the TWC as expected. By shifting combustion even leaner (lambda > 1.7) it was found that the engine out NO_X concentration could be reduced to a negligible amount.

Furthermore, study of increasing the HES is suggested as an option to limit the engine out HC emissions and place less of a demand on the TWC. There will however be a trade-off between the practicality of storing large amounts of H_2 on board a vehicle and the benefit of HC emissions reduction.

The significance of these findings is the potential to have large CO_2 emissions reduction whilst still operating the ICE which is a well-known and understood technology that already has significant market penetration. The abatement of emissions from this system when dual-fuelled with gasoline and H_2 will enable this technology to be taken forward through the further work suggested on different aftertreatment solutions and investigation of increased HES.

Acknowledgments

This work would like to acknowledge the financial support of the EPSRC- EP/W016656/1 Decarbonised Clean Marine: Green Ammonia Thermal Propulsion (MariNH3), the University of Birmingham for providing the PhD scholarship to M.Y. Johnson Matthey for providing the catalyst for the studies and their expertise.

References

[1] N. Rietmann, B. Hügler, and T. Lieven, “Forecasting the trajectory of electric vehicle sales and the consequences for worldwide CO2 emissions,” *J Clean Prod*, vol. 261, Jul. 2020, doi: 10.1016/j.jclepro.2020.121038.

[2] S. T. P. Purayil, M. O. Hamdan, S. A. B. Al-Omari, M. Y. E. Selim, and E. Elnajjar, “Review of hydrogen–gasoline SI dual fuel engines: Engine performance and emission,” *Energy Reports*, vol. 9. Elsevier Ltd, pp. 4547–4573, Dec. 01, 2023. doi: 10.1016/j.egyr.2023.03.054.

[3] B. Su, Y. Wang, Z. Xu, W. Han, H. Jin, and H. Wang, "Novel ways for hydrogen production based on methane steam and dry reforming integrated with carbon capture," *Energy Convers Manag*, vol. 270, Oct. 2022, doi: 10.1016/j.enconman.2022.116199.

[4] M. D. Scovell, "Explaining hydrogen energy technology acceptance: A critical review," *International Journal of Hydrogen Energy*, vol. 47, no. 19. Elsevier Ltd, pp. 10441–10459, Mar. 01, 2022. doi: 10.1016/j.ijhydene.2022.01.099.

[5] L. Rouleau, F. Duffour, B. Walter, R. Kumar, and L. Nowak, "Experimental and Numerical Investigation on Hydrogen Internal Combustion Engine," in *SAE Technical Papers*, SAE International, Sep. 2021. doi: 10.4271/2021-24-0060.

[6] Z. Yang, Y. Du, Q. Geng, and G. He, "Energy loss and comprehensive performance analysis of a novel high-efficiency hybrid cycle hydrogen-gasoline rotary engine under off-design conditions," *Energy Convers Manag*, vol. 267, Sep. 2022, doi: 10.1016/j.enconman.2022.115942.

[7] S. Pan, J. Wang, and Z. Huang, "Effects of hydrogen injection strategy on the hydrogen mixture distribution and combustion of a gasoline/hydrogen SI engine under lean burn condition," *Int J Hydrogen Energy*, vol. 47, no. 57, pp. 24069–24079, Jul. 2022, doi: 10.1016/j.ijhydene.2022.05.197.

[8] K. V. Shivaprasad, S. Raviteja, P. Chitragar, and G. N. Kumar, "Experimental Investigation of the Effect of Hydrogen Addition on Combustion Performance and Emissions Characteristics of a Spark Ignition High Speed Gasoline Engine," *Procedia Technology*, vol. 14, pp. 141–148, 2014, doi: 10.1016/j.protcy.2014.08.019.

[9] S. Wang, C. Ji, and B. Zhang, "Starting a spark-ignited engine with the gasoline-hydrogen mixture," *Int J Hydrogen Energy*, vol. 36, no. 7, pp. 4461–4468, Apr. 2011, doi: 10.1016/j.ijhydene.2011.01.020.

[10] Y. Du, X. Yu, J. Wang, H. Wu, W. Dong, and J. Gu, "Research on combustion and emission characteristics of a lean burn gasoline engine with hydrogen direct-injection," *Int J Hydrogen Energy*, vol. 41, no. 4, pp. 3240–3248, Jan. 2016, doi: 10.1016/j.ijhydene.2015.12.025.

[11] S. Wang, C. Ji, B. Zhang, and X. Zhou, "Analysis on combustion of a hydrogen-blended gasoline engine at high loads and lean conditions," in *Energy Procedia*, Elsevier Ltd, 2014, pp. 323–326. doi: 10.1016/j.egypro.2014.11.1116.

[12] D. Suresh and E. Porpatham, "Influence of high compression ratio and hydrogen addition on the performance and emissions of a lean burn spark ignition engine fueled by ethanol-gasoline," *Int J Hydrogen Energy*, May 2023, doi: 10.1016/j.ijhydene.2022.12.275.

[13] L. Wang, C. Hong, X. Li, Z. Yang, S. Guo, and Q. Li, "Review on blended hydrogen-fuel internal combustion engines: A case study for China," *Energy Reports*, vol. 8. Elsevier Ltd, pp. 6480–6498, Nov. 01, 2022. doi: 10.1016/j.egyr.2022.04.079.

[14] I. M. M. Elsemary, A. A. A. Attia, K. H. Elnagar, and A. A. M. Elaraqy, "Experimental investigation on performance of single cylinder spark ignition engine fueled with hydrogen-gasoline mixture," *Appl Therm Eng*, vol. 106, pp. 850–854, Aug. 2016, doi: 10.1016/j.applthermaleng.2016.05.177.

[15] R. Niu, X. Yu, Y. Du, H. Xie, H. Wu, and Y. Sun, "Effect of hydrogen proportion on lean burn performance of a dual fuel SI engine using hydrogen direct-injection," *Fuel*, vol. 186, pp. 792–799, Dec. 2016, doi: 10.1016/j.fuel.2016.09.021.

[16] S. Molina, S. Ruiz, J. Gomez-Soriano, and M. Olcina-Girona, "Impact of hydrogen substitution for stable lean operation on spark ignition engines fueled by compressed natural gas," *Results in Engineering*, vol. 17, Mar. 2023, doi: 10.1016/j.rineng.2022.100799.

[17] D. Suresh and E. Porpatham, "Influence of high compression ratio and hydrogen addition on the performance and emissions of a lean burn spark ignition engine fueled by ethanol-gasoline," *Int J Hydrogen Energy*, vol. 48, no. 38, pp. 14433–14448, May 2023, doi: 10.1016/j.ijhydene.2022.12.275.

[18] G. A. Karim, "Hydrogen as an engine fuel some pros and cons," *Journal of KONES Powertrain and Transport*, vol. 14, no. 4, 2007.

[19] I. T. YILMAZ, "The effect of hydrogen on the thermal efficiency and combustion process of the low compression ratio CI engine," *Appl Therm Eng*, vol. 197, Oct. 2021, doi: 10.1016/j.applthermaleng.2021.117381.

[20] M. Akcay, I. T. Yilmaz, and A. Feyzioglu, "The influence of hydrogen addition on the combustion characteristics of a common-rail CI engine fueled with waste cooking oil biodiesel/diesel blends," *Fuel Processing Technology*, vol. 223, Dec. 2021, doi: 10.1016/j.fuproc.2021.106999.

[21] J. Kim, K. M. Chun, S. Song, H. K. Baek, and S. W. Lee, "Hydrogen effects on the combustion stability, performance and emissions of a turbo gasoline direct injection engine in various air/fuel ratios," *Appl Energy*, vol. 228, pp. 1353–1361, Oct. 2018, doi: 10.1016/j.apenergy.2018.06.129.

[22] L. Wang *et al.*, "Experimental study on the high load extension of PODE/methanol RCCI combustion mode with optimized injection strategy," *Fuel*, vol. 314, Apr. 2022, doi: 10.1016/j.fuel.2021.122726.

[23] L. Chen, X. Zhang, R. Zhang, J. Li, J. Pan, and H. Wei, "Effect of hydrogen direct injection on natural gas/hydrogen engine performance under high compression-ratio conditions," *Int J Hydrogen Energy*, vol. 47, no. 77, pp. 33082–33093, Sep. 2022, doi: 10.1016/j.ijhydene.2022.07.176.

[24] D. E. Nieman, A. P. Morris, J. T. Miwa, and B. D. Denton, "Methods of Improving Combustion Efficiency in a High-Efficiency, Lean Burn Dual-Fuel Heavy-Duty Engine," in *SAE Technical Papers*, SAE International, Jan. 2019. doi: 10.4271/2019-01-0032.

[25] N. Gültekin and M. Ciniviz, "Experimental investigation of the effect of hydrogen ratio on engine performance and emissions in a compression ignition single cylinder engine with electronically controlled hydrogen-diesel dual fuel system," *Int J Hydrogen Energy*, vol. 48, no. 66, pp. 25984–25999, Aug. 2023, doi: 10.1016/j.ijhydene.2023.03.328.

[26] S. Molina, S. Ruiz, J. Gomez-Soriano, and M. Olcina-Girona, "Impact of hydrogen substitution for stable lean operation on spark ignition engines fueled by compressed natural gas," *Results in Engineering*, vol. 17, Mar. 2023, doi: 10.1016/j.rineng.2022.100799.

[27] F. Battin-Leclerc, "Detailed chemical kinetic models for the low-temperature combustion of hydrocarbons with application to gasoline and diesel fuel surrogates," *Progress in Energy and Combustion Science*, vol. 34, no. 4. Elsevier Ltd, pp. 440–498, 2008. doi: 10.1016/j.pecs.2007.10.002.

[28] Z. Fu, Y. Li, H. Chen, J. Du, Y. Li, and W. Gao, "Effect of Hydrogen Blending on the Combustion Performance of a Gasoline Direct Injection Engine," *ACS Omega*, vol. 7, no. 15, pp. 13022–13030, Apr. 2022, doi: 10.1021/acsomega.2c00343.

[29] V. Kärcher, P. Hellier, and N. Ladommatos, "Effects of Exhaust Gas Hydrogen Addition and Oxygenated Fuel Blends on the Light-Off Performance of a Three-Way Catalyst," *SAE Technical Paper*, vol. 2019-01–2329, 2019.

[30] Q. he Luo *et al.*, "Experimental investigation of combustion characteristics and NOx emission of a turbocharged hydrogen internal combustion engine," *Int J Hydrogen Energy*, pp. 5573–5584, Feb. 2019, doi: 10.1016/j.ijhydene.2018.08.184.

[31] A. Alagumalai, A. Jodat, O. Mahian, and B. Ashok, "NOx formation chemical kinetics in IC engines," in *NOx Emission Control Technologies in Stationary and Automotive Internal Combustion Engines: Approaches Toward NOx Free Automobiles*, Elsevier, 2021, pp. 39–68. doi: 10.1016/B978-0-12-823955-1.00002-4.

[32] F. Zeng and K. L. Hohn, "Modeling of three-way catalytic converter performance with exhaust mixture from natural gas-fueled engines," *Appl Catal B*, vol. 182, pp. 570–579, Mar. 2016, doi: 10.1016/j.apcatb.2015.10.004.

[33] B. Ling-zhi *et al.*, "Simulation and experimental study of the NOx reduction by unburned H2 in TWC for a hydrogen engine," *Int J Hydrogen Energy*, vol. 45, no. 39, pp. 20491–20500, Aug. 2020, doi: 10.1016/j.ijhydene.2019.10.135.

[34] R. J. Farrauto, M. Deeba, and S. Alerasool, "Gasoline automobile catalysis and its historical journey to cleaner air," *Nature Catalysis*, vol. 2, no. 7. Nature Publishing Group, pp. 603–613, Jul. 01, 2019. doi: 10.1038/s41929-019-0312-9.

[35] S. B. Kang, S. B. Nam, B. K. Cho, I. S. Nam, C. H. Kim, and S. H. Oh, "Effect of speciated HCs on the performance of modern commercial TWCs," *Catal Today*, vol. 231, pp. 3–14, Aug. 2014, doi: 10.1016/j.cattod.2013.11.032.